EUR-CEA-FC-1222 EUR-CEA-FC-1253

INFLUENCE OF PARTIALLY-STRIPPED IMPURITY IONS ON THE ION-CYCLOTRON ABSORPTION OF THE FAST MAGNETOSONIC WAVE IN TFR PLASMAS

TFR Group

November 1987

EURATOM

ASSOCIATION EURATOM - C.E.A.

DEPARTEMENT DE RECHERCHES SUR LA FUSION CONTROLEE

By including heavy impurity ions in the wave propagation equa-

TREC-SCP-STUI EUR-CEA-FC-1083

INFLUENCE OF PARTIALLY-STRIPPED IMPURITY IONS ON THE CYCLOTRON ABSORPTION OF THE FAST MAGNETOSONIC WAVE IN TFR PLASMAS

TFR Group

November 1982

Submitted for publication to Nuclear Fusion

INFLUENCE OF PARTIALLY-STRIPPED IMPURITY IONS ON THE CYCLOTRON ABSORPTION OF THE FAST MAGNETOSONIC WAVE IN TFR PLASMAS

TFR GROUP*

ASSOCIATION EURATOM-CEA SUR LA FUSION
Département de Recherches sur la Fusion Contrôlée
Centre d'Etudes Nucléaires
Boite Postale n°6. 92260 FONTENAY-AUX-ROSES (FRANCE)

ABSTRACT

Injection of vanadium ions by the laser blow-off technique has permitted to modify at will the impurity content in TFR plasmas prior to ion-cyclotron resonance (ICR) heating experiments in the mode conversion regime. The initial rate of increase of the central deuteron temperature $T_D(0)$ has thus been enhanced. By solving the wave propagation equation in the WKB approximation, it has been possible to account for the enhanced $dT_D(0)/dt$ value by wave energy deposition on resonating V^{21+} ions, provided a fraction (of the order of 10 %) of these ions has been accelerated to the tens of keV range. Previous experimental ICR heating results, in conditions such that the proton cyclotron layer is outside the limiter radius, can be explained by similar resonance processes on intrinsic metal impurity ions.

I - INTRODUCTION

The application of radio-frequency electric fields at the ion-cyclotron resonance (ICR) in Tokamak plasmas is a promising method to reach ignition and is currently under intensive experimental investigation. However, a variety of resonances, cut-offs and modes exist near the ion-cyclotron resonance ; consequently the physics of wave absorption is quite complex [1] . In this article, we focus our analysis on the role played by impurity ions in the wave absorption mechanism.

ICR heating antennas are designed to couple the RF power to the plasmas particles via the compressional wave mainly propagating perpendicularly to the magnetic field lines. For the TFR experiments discussed in this paper, the antenna was located on the high magnetic field side of the torus, in order to investigate ICR heating in the mode conversion regime [2]. It has been observed that, in a two-ion (H and D) plasma, the optimum heating effect is achieved when the hybrid layer is located on the magnetic axis. The energy of the wave is then damped by the thermal motion of electrons, via Landau damping in the vicinity of the hybrid (mode conversion) layer, and by the motion of minority protons via cyclotron damping at their fundamental ICR location. Evidence for such absorption lies not only on both electron and majority deuteron heatings, but also on the observation of suprathermal electrons, on the existence of a fast proton tail and on the spectral analysis of coherently scattered light [3] .

The TFR experiments were designed to study ICR heating effects at large values of the hydrogen isotope ratio $\eta_H = n_H / n_D$ ($\eta_H \cong 0.2 - 0.5$). By increasing η_H and B_T (the toroidal magnetic field) simultaneously (thus keeping the location of the hybrid layer at the plasma center) the proton cyclotron resonance layer could be progressively removed from the vacuumm chamber. In these conditions, the non-Maxwellian proton tail should disappear and the wave energy should be mainly absorbed by Landau damping on electrons. This is indeed experimentally observed ; however, a significant heating of deuterons is still observed [4] , which is difficult to justify on the basis of a simple wave propagation model [3] . Additionally, when the plasma isotopic composition η_H was chosen in such a way that the two-ion hybrid layer location is both slightly shifted towards

the low magnetic field side and coincident with the second harmonic cyclotron frequency of partially stripped He-like Ar ions (Ar being purposely injected into the discharge), the ICR pulse efficiently pumped out the argon impurities, thus effectively cleaning the discharge [5]. Noticeably, when this effect takes place the electron temperature does not increase, while the ion temperature increase appears to depend on the location of the hybrid layer inside the plasma.

The above experiments used inconel limiters and lateral antenna protections, and were characterized by a relatively large amount of metallic impurities. Subsequently, carbon limiters and lateral antenna protections were installed, resulting in a considerable reduction of metallic impurities in both ohmic and ICR-heated plasmas [6]. This also changed the electron and deuteron temperature behaviour during ICR heating. In particular, the rate of increase of the central deuteron temperature is now lower (figure 1) : at a coupled RF power of 300 kW, $dT_D(0)/dt = 16$ eV ms^{-1} for the inconel configuration (curve a) and 12 eV ms^{-1} for the carbon one (curve b).

All these observations suggest that heavy impurities may play an important role in the mechanism of RF energy transfer. The effect of heavy ions on the RF power balance has been theoretically analysed by Longinov and Stepanov [7]. They considered a two-ion (H and D) plasma for which the mode conversion layer is located in the bulk of the discharge, and pointed out that a large fraction of the RF power could be absorbed by heavy ions (a third ion species) if their second harmonic resonance layer is located in the vicinity of the mode conversion layer. Heating of the bulk plasma ions is then due to equipartition with the hot admixture ions. Quantitatively, Z-times ionized ions result in the same heating efficiency than the proton minority for a density Z^2 times as low. They have also shown theoretically, the formation of a high energy tail with a high energy cut-off for the resonating, energy absorbing, ions [8].

To clarify these experimental observations and theoretical suggestions, we have purposely modified the heavy ion content during ICR heating experiments on TFR. Using the laser blow-off technique [9,10] vanadium ions were injected in the centre of the discharge just before or

during the RF pulse. It should be noted that an experiment along the same lines has been recently performed on T-10, by injecting the neon isotope of atomic mass 22 [11].

This article is organized as follows. After a description of the experimental results in section 2, section 3 discusses the location of the second harmonic resonances and the radial density profiles of impurity ions. Section 4 explains the experimental results, most of the interpretation being based on the results of a numerical code solving the wave propagation equation in the WKB approximation. Finally, in section 5 we shall consider the role of intrinsic impurities.

II - EXPERIMENTAL RESULTS

ICR heating experiments in the mode conversion regime, using a high magnetic field side antenna, have been previously described [2,12]. The present experiment was carried out on the following target plasmas : plasma current I_p = 250 kA, toroidal field B_T = 4.5 T, carbon limiter radius a = 19 cm, central electron density $n_e(0) = 10^{14}$ cm^{-3}, central electron temperature $T_e(0)$ = 1.5 keV, and central ion temperature $T_D(0)$ = 0.9 keV. Mode conversion ICR heating was obtained by adjusting the hydrogen isotope ratio to $n_H = 0.2$. In these conditions, the hybrid layer is located on the magnetic axis. Typically 100 ms, 60 MHz, 600 - 800 kW RF pulses were applied to the plasma at the current plateau. They resulted in electron density increases of 15-20 %, with central temperature heatings $\Delta T_e(0)$ and $\Delta T_D(0)$ of the order of 150-300 eV [13] and with simultaneous degradation of the energy confinement time. Figure 2a shows the radial profiles of n_e, T_e, and T_D, obtained from standard diagnostics during the second half of the RF pulse, when practically steady-state conditions are attained.

Several Ni, Cr and Fe lines were routinely monitored in the v.u.v spectral region, and used to evaluate the heavy impurity content of the discharge [14]. The ohmically heated target plasma described above had central total ion densities of 2×10^9 cm^{-3}, 10^9 cm^{-3}, and 0.8×10^9 cm^{-3} for Ni, Cr, and Fe, respectively. The metallic impurity content increased by approximately a factor of 5 during the RF pulse.

Fully ionized light impurity (oxygen and carbon) densities were measured in the ohmic plasmas by charge-exchange recombination spectroscopy [15] ; however, they were only slightly modified by ICR heating. Densities of 1.5×10^{12} cm^{-3} and 10^{12} cm^{-3} were obtained for central fully ionized carbon and oxygen ions, respectively. Moreover radial emissivities of the hydrogen-like light impurity ion lines are also routinely obtained. The densities of these ions have a shell-like structure peaking at radii $r \cong 12$ cm for oxygen and $r \cong 14$ cm for carbon ; however, the impurity transport simulation code indicates that residual H-like ion densities of the order of 10^9-10^{10} cm^{-3} exist at the plasma centre.

A sudden increase of the plasma impurity content was performed by injecting a vanadium puff by the laser blow-off technique [9,10]. The vanadium evolution in the plasma was followed by using two grazing incidence spectrometers and a X-ray crystal spectrometer (see [16] for more details). The quantity of injected vanadium is chosen in such a way as to leave the main parameters of the ohmic plasmas unaffected. Furthermore, the time behaviour and amplitude of the vanadium ion radiances are not modified under the effect of the RF power, indicating that the impurity transport properties do not change [16]. Numerical impurity transport simulations [17] (using an anomalous flux, characterized by a diffusion coefficient D_A and a convective coefficient V_A, having typical TFR plasma values, i.e., $D_A = 4000\ cm^2 s^{-1}$ and $V_A = 800\ cms^{-1}$) show that the total V-ion density profile becomes peaked on axis about 15-20 ms after the injection (with a maximum central density of $\sim 5 \times 10^{10}\ cm^{-3}$) and then relaxes with a time constant of approximately 40-50 ms. Simulated profiles of several V ions, 20 ms after injection, are shown in figure 2b ; the most abundant ions in the plasma centre are V^{21+} and V^{20+} (He-like and Li-like isoelectronic sequences, respectively).

The V injection has no effect on most of the diagnostics (e.g., n_e and T_e) for both ohmic and ICR-heated plasmas. However, this is not the case for the ion temperature diagnostics. The central deuteron temperature is deduced from neutron emission and charge-exchange energy analysis ; its time evolution is shown in figure 3 (a and b, respectively). The experimental observations can be summarized as follows. (i) If the V injection occurs during the ohmic phase (no RF pulse ; figures 3A, curve 1), no noticeable effect can be detected on the deuteron temperature. (ii) When the V injection occurs 20 ms before the RF pulse, such that enough time has elapsed for the radial profile of the total V-ion density to reach a peaked shape, both diagnostics show that the $T_D(0)$ initial growth rate is larger than the corresponding one without V injection (figures 3A, curves 3 and 2, respectively). However the asymptotic $T_D(0)$ value is the same in both cases. It was initially thought that this is due to the fact that, 60-70 ms after the V injection, the total V-ion density profile has almost completely relaxed. (iii) To test this assumption, V was injected 20 ms after the beginning of the RF pulse, before $T_D(0)$ reached its asymptotic

value (figures 3 B). Although a slight difference in the $T_D(0)$ time evolutions can be seen (compare curves 3 and 2), no modification in its asymptotic value could be detected (but now central V ions are present with considerable density up to the end of the RF pulse). Since the same amount of V ions was injected in both cases, and the RF power delivered by the antenna is unaffected by the V injection, the constant $T_D(0)$ saturation value must be attributed to a further degradation of the energy confinement time τ_E. It should be noted here that the present $T_D(0)$ saturation behaviour is markedly different from the T-10 results [11], where Ne injection has allowed to roughly double the deuteron temperature increase induced by the ICR heating with respect to the no Ne injection case. Although no spectroscopic data can be found in the paper of Alikaev et al. [11], it is well known that Ne, similarly to all noble gases [5], is a recycling element and that is very likely to modify the characteristics of the target ohmic plasma (thus possibly explaining the different deuteron temperature behaviour).

III - IMPURITY ION RESONANCES

In the light of the above observations, we wish to show in the following that a large fraction of the RF power can be directly absorbed via second harmonic cyclotron damping on the impurity ions when ICR heating is applied to a hot 2-component (H and D) plasma containing an impurity ion species, provided that the hybrid layer of the two main plasma ions coincides with (or, at least, is near to) the second harmonic cyclotron resonance of the Z-times ionized impurity ions. The bulk of the plasma is then heated, via Coulomb collisions, by the fraction of the impurity ions which have absorbed the RF energy.

The first step is to locate, for given experimental conditions (i.e., B_T and η_H values), the position of the resonances of a given atomic species. A supplementary condition is, of course, the existence of these ions, at the resonance location, this being determined to first order by the T_e radial profile (a more precise calculation would have to consider also the impurity transport).

Figure 4 shows, for several impurity elements of nuclear charge Z_N (upper abscissa scale), the ratio of the second harmonic cyclotron frequencies f_{2cZ} to twice the proton cyclotron frequency f_{cH} (left ordinate scale) ; this ratio is simply equal to the charge over mass ratio Z/A (we have chosen for each element the mass A of the naturally most abundant isotope). Different isoelectronic sequences (from fully stripped to Be-like ions) are identified by different symbols (the lines joining them being only a visual aid).

To locate these resonances with respect to the hybrid layer position, we consider a three-ion plasma (majority deuterons, with minority protons and fully ionized carbon ions, having density ratios with respect to deuterons η_H and $\eta_{C^{6+}}$; heavy impurities can here be neglected, since their low density does not modify the structure of the dispersion relation). The ratio of the hybrid frequency f_{Hy} to twice the proton cyclotron frequency f_{cH} (calculated in the cold plasma approximation, without inclusion of the parallel refractive index) is also plotted in figure 4 (solid thick lines, with ordinate scale to the right) as a function of $\eta_{C^{6+}}$ (lower abscissa scale), for two values of η_H.

It will be shown in the following section that, for absorption at the impurity ion resonances to be effective, the resonance layer must be located near the hybrid layer on the high magnetic field side. Therefore, as a consequence of the 1/R dependence of B_T, for each thick solid line (i.e, at a given n_H value) the most important ions, as far as RF absorption is concerned, are those just below the curve. These considerations led to the choice of parameters for the Ar pump-out experiment [5], since figure 4 shows that for He-like Ar ions the resonant and hybrid layer coincide at $n_H \cong 0.5$.

As far as the experiments reported here are concerned, we must consider the $n_H = 0.2$ curve and V ions. It appears that the resonance of the most abundant He-like ions is correctly located (the H-like ion resonance is nearer to the hybrid layer, but the central density of these ions is negligible at the electron temperature of TFR plasmas).

Fully-stripped light element ions (O^{8+} and C^{6+}) have cyclotron resonances coincident with the proton cyclotron layer ($f_{2cZ}/2f_{cH} = 0.5$) ; therefore, they are above the $n_H = 0.2$ curve and do not contribute to the absorption under discussion. On the other hand, H-like light element ions (having at the plasma center small, but not completely negligible, densities, as shown by the numerical impurity transport code) are correctly located to influence the RF wave propagation at $n_H = 0.2$. It should also be mentioned that-fully stripped ions of naturally less abundant C and O isotopes (of mass 13 and 18, respectively) have Z/A values similar to those of the H-like ions of the most abundant isotopes ; they could therefore, play a role in the absorption of the wave . It was for this reason that experiments on T-10 used the Ne isotope of mass 22 rather than the more abundant one of mass 20.

Finally, the influence of intrinsic metal impurity ions will be discussed in section 5.

IV - ENERGY TRANSFER AND POWER BALANCE

In view of the previous considerations, we consider a plasma composed of electrons, deuterons, protons, fully-stripped ions of a light element (C^{6+}) and partially stripped ions of the injected heavy element (V^{21+}) ; the different minority ions are characterized by their relative densities n_i with respect to the majority deuterons.

The presence of C^{6+} and V^{21+} impurity ions in the plasma does not appreciably affect the overall structure of the wave dispersion function. Indeed, C^{6+} impurity ions have the same charge to mass ratio as deuterons, therefore, the hybrid layer, lying between the cyclotron resonances of hydrogen and deuterium, can only be slightly shifted towards the location of the cyclotron resonance of protons (as shown by the thick solid lines of figure 4). Furthermore, since the concentration of V^{21+} ions is less than (10^{-3} - 10^{-4}) n_D, they only result in a negligible perturbation in the wave dispersion response of the plasma.

IV.1 - 0-D simulation of central T_D and T_e temperatures

The simplest quantitative analysis can be obtained by using a zero-dimensional code describing the behaviour of the central plasma [13]. In the frame of this analysis, particles exchange energy by Coulomb collisions (P_{eq}), and each species can absorb or lose energy independently (P_{Ω}, P_{RF}, P_{rad}, P_{cx}, power lost during an internal disruption) ; conduction and convection losses are globally represented by an energy confinement time for each component.

For the experimental conditions during ICR heating ($T_e(0)$ = 1.7 keV, $T_H(0) = T_D(0) = T_{C^{6+}}(0) = T_{V^{21+}}(0)$ = 1.2 keV, $n_e(0)$ = 1.2 x 10^{14} cm^{-3}, $n_D(0)$ = 10^{14} cm^{-3}, $n_H(0)$ = 2 x 10^{13} cm^{-3}, $n_{C^{6+}}$ = 2 x 10^{12} cm^{-3}, $n_{V^{21+}}$ = 4 x 10^{10} cm^{-3}), the shortest equipartition times are for collisions of V^{21+} ions with C^{6+} and D^+ ions. Consequently, in the frame of the 0-D simulation, if an extra-amount of RF power is absorbed by the V^{21+} ion population, the global RF efficiency will appear larger due to the strong energy transfer to C^{6+} and D^+ ions (these two ion populations being also strongly coupled together).

The $T_e(0)$ and $T_D(0)$ evolutions of the reference ICR-heated discharge without V injection (curves 2 of figures 3) could be simulated by giving a RF power density of 1.2 W cm^{-3} to the electrons and of 0.4 W cm^{-3} to the minority protons (deuterons being heating indirectlly through collisions). However, in order to correctly simulate the central temperature evolution when vanadium was injected just before the RF pulse (curves 3 of figure 3A), an additional power density of 0.25 W cm^{-3} had to be given to the V^{21+} population. This extra power density is only applied during 40 ms, roughly corresponding to the full-widths at half maximum of the radiances of the central vanadium ions. A slightly less extra power density must be given to the V^{21+} ions to simulate the case of V injection during the RF pulse (curve 3 of figure 3B) ; however, in order to correctly follow the $T_D(0)$ saturation, the deuteron energy confinement time must be reduced (with respect to the reference ICR-heated discharge) after $\sim$ 20 ms (alternatively, the deuteron energy confinement time can be kept constant as in the previous simulation, but then the extra power density must be applied only during $\sim$ 20 ms, i.e. much less than the V^{21+} ion "life-time" in the central plasma).

Implicit in this model in the approximation that the entire population of V^{21+} ions is accelerated by the RF field in such a way that its distribution function remains Maxwellian. This approximation is, however, not necessary, and the experimental results can also be simulated by the equivalent of a fast tail containing 10 % of the total V^{21+} population.

IV.2 - ICR wave propagation in a multicomponent plasma

As it will be shown below, V^{21+} cyclotron absorption from the fast magnetosonic wave (before mode conversion) can be neglected. Additionally (see Appendix), in a D plasma containing a V^{21+} impurity of very low concentration ($n_{V^{21+}} < 10^{-3}$) the hybrid layer mode conversion process due to vanadium is also not important. Therefore, in the mode conversion regime V^{21+} ions absorb energy only via second harmonic absorption requiring short perpendicular wavelengths associated with Bernstein waves. In the region where the ion Bernstein wave exists, the impurity ions are in competition with electrons as far as absorption is concerned. We shall now show, by solving the wave propagation equation, that all these processes are indeed possible.

The numerical code used to justify the RF power density absorbed by the V ions considers a slab model propagation of the wave field along the major radius direction x in the WKB approximation [18,19]. The warm plasma dielectric tensor is evaluated at each point of an inhomogeneous plasma having 7 independent ion species (plus electrons) of constant ion density η_i with respect to majority deuterons. Refraction is neglected, but the components of the dielectric tensor are computed in a frame linked to the field lines, in order to take into account the influence of the rotational transform. Parameters to be specified are the wave number $k_{\parallel}$ along the toroidal field direction z and the "probing" chord height y along the vertical direction. The plasma parameter profiles are specified by analytical fits of the experimental curves, while the radial density profiles of the most important heavy impurity ions are deduced from numerical calculations of the impurity transport. Central fully-stripped light impurities (important for their influence on the hybrid layer location, but not for absorption) are globally simulated by $\eta_{C^{6+}} = 3 \times 10^{-2}$. Absorption by H-like light impurity ions, by their fully-stripped heavier isotopes and by intrinsic metal ions is not included in the simulation of the V injection experiments (see later for a discussion of their effect).

The code evaluates also the local absorption (it actually evaluates the imaginary part of the wave number k_i (x)) of each species and the integrated (along the trajectory up to x) fractional absorbed power $F_a(x)$. It does not include tunnelling of the fast wave through the evanescence region between the fast wave cut-off and the ion-ion hybrid layer. Consequently, only excitation from the high magnetic field side ($x = -\infty$) is possible ; however, this corresponds to the experimental situation on TFR.

It is well known that for a two ion (H and D) plasma, at y = 0, the fast wave incident from the high magnetic field side is reflected back at the hybrid layer central location and converted into a slow wave absorbed by electrons. Figure 5 shows the influence on the hybrid layer location (turning point of the dispersion curve) of varying $k_{\parallel}$, $\eta_{C^{6+}}$, and y. For larger values of y (above 5-10 cm), the effect of the rotational transform is so important that the slow wave direction is inverted, and propagation towards the proton cyclotron layer on the low magnetic field side is possible, resulting in cyclotron absorption by minority protons.

By including heavy impurity ions in the wave propagation equation, it is possible to cross additional second harmonic resonances, thus increasing absorption with respect to the simple case discussed above. In view of explaining our experimental results, V^{21+} and V^{20+} ions (with n_i values of 10^{-3} and 5×10^{-4}, respectively) have been included in the calculations shown in figure 5 ; however, their concentrations are too low to affect the structure of wave propagation (i.e., the real part of the wave number k_x is determined essentially by two-ion H/D processes). This is not the case for absorption, since the slow wave can be absorbed by impurity ions at resonance. Considerable absorption however requires increasing the V ion temperature T_V by a large factor α (i.e., $T_V = \alpha T_D$), well above the T_D value ; the required α value is a function of the distance between the turning point and the impurity ion resonance. Since the fraction of accelerated V ions is unknown (see later for further considerations), we have performed a few calculations by reducing the fraction of resonating ion for which $\alpha >> 1$, in view of determining a lower limit for the accelerated ion fraction. An example is shown in figure 6. The left figure shows the coefficient $k_i(x)$ for the fast and slow waves for both electrons and V ions. The dot-dashed and solid lines (for the fast and slow wave, respectively) are obtained by taking $\alpha = 40$ for both V ions, they indicate that the V ion resonance absorption is weak for the fast wave and important for the slow wave when the second harmonic layer is approached. The dotted and dashed lines (also for the fast and slow wave, respectively) are obtained by taking $\alpha = 1$ for both ions but adding 10 % of fast V^{21+} and V^{20+} ions with $\alpha = 40$; they clearly show that it is not necessary to deform the distribution function of all the resonating V ions to obtain important absorption. The right part of figure 6 shows the integrated fractional absorbed power $P_a(x)$ from the slow wave for both electrons and V^{21+} ions. In the examples shown, approximately 20 % of the energy is absorbed by electrons, the rest ($\sim$80 %) going to V^{21+} ions.

Extensive calculations have indicated that important absorption by V^{21+} ions is always possible, provided that electron absorption has not become the dominant process for slow wave energy depletion before the impurity resonance layer is reached. In this context, it must be stressed that all parameters displacing the turning point towards the low magnetic field side favour electron energy absorption : figure 7 shows the effect of increasing the "probing" chord height y, and figure 8 shows the effect of varying the wavenumber $k_{\parallel}$ at a few y values.

IV.3 - Transfer of the energy absorbed by V ions

The estimated important absorption by V^{21+} ions implies a deformation of the distribution function near the absorbing resonant layer. Although no experimental evidence exists for such an effect in the present experiments, it has been predicted theoretically by integrating the Fokker-Planck (quasi-diffusion) equation for the resonating species distribution function. Second harmonic heating was considered for deuterium by Krapchev [20], and for fully ionized Ne ions by Longinov et al [8]. It should also be pointed out here that Monte-Carlo calculations [19,21] have indicated that both minority protons and impurity ions, gaining energy discontinuously in the resonance layer, can be accelerated up to the 100 keV energy range. The impurity calculations were performed for He-like Ar^{16+} ions (because of the pump-out experiment [5]), but they are of general validity ; depending on the particular experimental conditions, the accelerated particles can either transfer their energy to the plasma or be lost by trajectory effects.

The wave propagation code has shown that impurity induced absorption is localized in narrow layers ($\sim$ 1 cm thick ; see figures 6 and 7) ; the energy gained by the resonating particles is then smeared out over the central plasma region by the drift of the guiding centers, as shown by Monte-Carlo trajectories (incidentally, this also happens for the minority protons heated in their non-central first harmonic resonance layer). Coulomb collisions of "hot" V ions with the other plasma components then allow the absorbed RF power to be transferred to the plasma.

In order to determine how the perpendicular energy gained by V ions is redistributed among the different species, we consider the energy loss rate of a V^{21+} test particle with velocity v

$$\frac{d}{dt} v^2 (V^{21+}) = - v^2 (V^{21+}) / \tau (V^{21+}, i)$$

where $\tau (V^{21+}, i)$ is the energy-exchange time [22] between the V^{21+} test particle and a field particle i (i = H^+, D^+, C^{6+}, V^{21+}, e). The values of τ for the conditions of the present experiment are given in Table I. In the energy range 1.2-40 keV, the test particle loses its energy preferentially to D^+ and C^{6+} ions, and to a lesser extent to H^+ ions.

These considerations also show that V ions are unlikely to be heated by interaction with the fast proton tail. Indeed, at the given V density the energy exchange time between H^+ and V^{21+} ions is of the order of 0.1 s. Such a long exchange time makes very unlikely that deuterons be more efficiently heated in the presence of V ions, if the V ions are not directly heated. We are therefore led to reject the scenario where the V ions would be rapidly heated by the proton tail, followed by thermalization with deuterons in order that the net result be an increase of the $dT_D(0)/dt$ slope at the onset of the RF pulse.

The value of the power density given to V ions has been estimated by the 0-D simulation (subsection IV.1) ; we must now verify that the absorbed power can be effectively transferred to majority deuterons by Coulomb collisions. If $\tau_{eq}\ (V^{21+},\ D^+)$ is the equipartition time [23] between V^{21+} and D^+ ions with temperatures, T_V and T_D, respectively, the balance equation for V^{21+} ions at steady state is (neglecting any other energy loss)

$$P_{ICR} = P_{V^{21+}/D^+} = \frac{3}{2}\ \frac{T_V - T_D}{\tau_{eq}(V^{21+},\ D^+)}\ ,$$

where P_{ICR} is the absorbed power density per unit V^{21+} ion density. The rhs of this expression has been plotted in figure 9 (solid line), taking $n_D = 10^{14}\ cm^{-3}$ and $T_D = 1.2$ keV. $P_{V^{21+}/D^+}\ (T_V)$ has a maximum for :

$$T_V = 2\ (\frac{m_V}{m_D} + 3)\ T_D \simeq 2\ \frac{m_V}{m_D}\ T_D,$$

where m_V and m_D are the masses of the two interacting particles. If we assume that the accelerated ions "equilibrate" themselves at this temperature, a "hot" V^{21+} ion density of approximately $1.5 \times 10^9\ cm^{-3}$, "diluted" over the central region, is necessary to transfer a power density of 0.25 W cm^{-3} (the value estimated in sub section IV.1). Note that this density value is quite plausible since it is only roughly 1/15 - 1/20 of the density given by v.u.v. spectroscopy.

In view of the following section, figure 9 also shows (dotted line) the corresponding function P_{C^{5+}/D^+} for C^{5+} ions as a function of the

C^{5+} ion temperature T_C. The shape of the curve does not change but the maximum value is reduced (by approximately the square of the charge ratio, i.e., a factor of $\sim$ 20) and it is attained at a lower temperature (by the mass ratio). Therefore, light ions are "resonantly heated" by the ICR wave less than heavy ions and, moreover, they are also less effective to transfer the RF power.

V - ABSORPTION BY INTRINSIC IMPURITIES

Intrinsic light impurities (C and O) when using carbon limiters, have in TFR densities of the order of 10^{12} cm^{-3} [15] (note that, when using inconel limiter, the O-ion density was also in the 10^{12} cm^{-3} range [24]). Since these light elements are completely ionized at the plasma center, their naturally most abundant isotopes have Z/A = 0.5, and their resonant layers coincide with the proton cyclotron layer, thus being not affected (or at least much less than protons) by the slow wave. Nevertheless, percentages of the order of 1 % of either partially stripped H-like ions (as predicted by the impurity transport code) or fully-stripped isotopes of larger mass (naturally less abundant) can be located in the central region near the hybrid layer. The numerical code of subsection IV.2 shows that appreciable absorption of the wave can then be effectively obtained if the density of these ions is of the order of 10^{10} cm^{-3} ; however, figure 9 also shows that they are "less heated" and are less effective than heavy impurities in coupling the RF power to the majority deuterons.

As far as intrinsic heavy impurities are concerned, nickel has always been in TFR the most abundant element [14,17,25] , both in ohmic and ICR-heated plasmas. As an example, we have analyzed (along the lines discussed in subsection IV.2) Ni-ion second harmonic resonance absorption when varying the η_H ratio between 0.2 and 0.5 at constant toroidal field B_T = 4.9 T (the experimental situation reported by Equipe TFR in Refs.- [4,25]). The radial profiles of the most abundant central Ni ions, calculated by the impurity transport code at the time of maximum deuteron temperature T_D (i.e., 30 ms after the Rf pulse application), are shown in figure 10. Figure 11a shows, for four η_H values, the dispersion curves k_x = f(x), along with the positions of the second harmonic resonance layers of the relevant Ni ions. The total integrated fractional absorbed powers $P_a(\infty)$, as functions of $k_{//}$, are shown in figure 11b. These calculations clearly indicate that the absorbing ions are always located either at the hybrid layer (turning point of the dispersion curve) or on its high magnetic field side. When two ions contribute to the absorption (e.g., at η_H = 0.3, the Li-like and Be-like ions), P_a (∞) is larger for the ion having its resonant layer nearer to the turning point. As in the V injection case, the absorbing ion temperature T_{Ni} has been increased by a

factor $\alpha = 40$ with respect to the deuteron temperature T_D. All cases shown in figure 11 indicate large absorption ; however, this can only be obtained if the absorbing resonant ions exists at their resonant layer, and this is not the case at $n_H = 0.2$, since the He-like Ni ion density is negligible at $x = + 9$ cm (see figure 10). Incidentally a more complete simulation of the experimental situation should also include the contribution of Fe and Cr ions.

For the same series of experiments figure 12 shows the experimental values of the maximum deuteron temperature increase $\Delta T_D(0)$ during the RF pulse and of its rate of increase $d T_D(0)/dt$ at the RF pulse application, as function of n_H ($P_{RF} = 650$ kW). Optimum heating conditions are clearly obtained at $n_H = 0.4$, when the hybrid layer is central. Since at $B_T = 4.9$ T the proton cyclotron layer is outside the limiter radius, it is possible that (as initially suggested in [4]) all the observed majority deuteron heating is a consequence of metal ion absorption. As expected much lower values of both $T_D(0)$ and $dT_D(0)/dt$ are obtained at $n_H = 0.25$, due to the combined effect of non-central energy deposisiton and lower resonanting impurity ion density at the hybrid layer. We should also mention here that in the same series of experiments (at constant RF power and toroidal magnetic field) it was observed that the Ni XVIII 292 Å radiance (monitor of the metal impurity content) is approximately constant for $0.35 \leq n_H \leq 0.5$, but is considerably increased for $n_H \leq 0.25$ [25] . Although the origin of metal impurities during ICR heating is by no means a completely understood subject, it is thought that they are due to deposition of some of the RF power (by an unclear mechanism) in the outer regions [26] . It is then possible that the increased nickel production at the lowest n_H value is due to the fact that, less RF power being absorbed by the plasma, more power is deposited in the outer region (it is indeed a general fact in TFR that every time that the RF power is less effectively absorbed by the core plasma, more metal impurities are produced).

VI - CONCLUSION

By injecting vanadium impurities into ICR-heated plasmas, it has been shown that V^{21+} ions absorb directly a fraction of the RF power via ion-cyclotron absorption at the second harmonic resonance. Calculations indicate that this requires a fast ion tail ; the V^{21+} ions, accelerated locally at the resonance, subsequently spread over the central region by trajectory effects (drifting of their guiding center) and then heat the majority deuterons by Coulomb collisions. No experimental evidence of the existence of this tail is available. As a result of the direct RF power absorption by V ions, the initial rate of increase of the deuteron temperature $dT_D(0)/dt$ is larger, but the $T_D(0)$ saturation value is not changed. This saturation behaviour is not understood, but the simulations require that, when injecting V during the RF pulse, the deuteron energy confinement time be further decreased.

In the light of the experiments, we have also considered the effect of intrinsic impurities on ICR heating. The calculations of section 5 have been repeated for the frequently occurring experimental situation of $\eta_H = 0.2$ and $B_T = 4.5$ T. They have shown that the resonantly absorbing metal ions belong to isoelectronic sequences existing in the plasma center, and that the "efficiencies" of these atomic species, as far as impurity induced ICR absorption is concerned, are comparable to that of V ions. The larger rates of increase of T_D observed in the case of an inconel environment (figure 1) could be due to the larger metal impurity content in the ohmic phase for these experimental conditions. Light impurities (carbon and oxygen) have also been considered but they are less effective than heavy metal ions.

The discussion of section 5 has indicated that impurity induced ICR absorption can effectively heat the majority deuterons even when the proton cyclotron layer is located outside the plasma ; such heating effects have indeed been observed both on TFR [4] and on T-10 [11]. It is therefore crucial that ICR heating experiments pay attention to the heavy (and possibly also light) impurity content of the plasma, in order to evaluate the absorption efficiency on their ions. This can be done by : i) determining the location of the second harmonic layer of impurity ions ; (ii) computing the impurity density and checking that the structure of the

wave dispersion relation is not changed ; (iii) considering the state of ionization of impurities located on the high magnetic field side of the hybrid layer, (iv) determining the maximum power that may be absorbed by the impurities ; and (v) evaluating the amount of power coupled to the majority ions due to the presence in the discharge of heavy impurities.

ACKNOWLEDGEMENTS

The authors wish to thank Dr. Y. Lapierre for fruitful discussions and for his help at the beginning of the utilization of his numerical code.

APPENDIX

Slow wave absorption at the impurity ion second harmonic

Second harmonic heating in a one-component plasma has been investigated experimentally on PLT and JFT-2M [27,28] , with the aim to study the absorption of the magnetosonic wave near the second harmonic of the ion species. It was shown that the net ICR effect was to produce an anisotropic ion tail in the direction perpendicular to the magnetic field. In fact, second harmonic heating involves in the plasma dispersion properties the argument $k_\perp \rho_L$, where $k_\perp$ is a representation of the perpendicular gradient of the electromagnetic field and ρ_L the particle Larmor radius. When a particle enters the resonant zone ($\omega = 2\,\omega_c$) it gains some perpendicular energy and ρ_L increases ; therefore, if this extra energy has ; not been damped by Coulomb collisions on its trajectory, the next time the particle enters the resonant layer it receives a larger energy increment. The second harmonic net heating effect, when combined with collisions, is therefore to sustain a tail [20] .

The picture is more complex when considering a two component plasma where both the fundamental resonance of species 1 and the second harmonic cyclotron resonance of species 2 are present in the plasma. There is then a natural competition between the hybrid layer resonance and the second harmonic resonance. Depending on the value of the ratio $n = n_1 / n_2$ and of the temperature of the bulk plasma, the hybrid layer mode conversion process or the harmonic resonance absorption will dominate. The second process is more important when n is low or β ($= v_{th}^2 / v_A^2$, v_{th} and v_A being the thermal velocity and Alfven velocity, respectively) of the bulk ions is large. This can be deduced in the frame of the WKB approximation. Considering the asymptotic part of the dispersion equation, it is possible to derive the coefficient δ which rules the set of transmission-reflexion coefficients associated with the mode conversion process [29,30] . Keeping only the terms associated with the fundamental resonance of species 1 and with the harmonic resonance of species 2, it can be shown that δ is essentially proportional to the sums of two terms A and B, where A represents the effect of the hybrid resonance and B the effect of the second harmonic. For a D/H plasma,

$$A = \frac{\eta}{4\beta_D} \frac{1/3 + \eta/4 - P^2}{1 + \eta/2 + P^2}$$

$$B = 1 - \eta + \frac{1}{2}\left[(P^2 + 1/3 + \eta/8)(1 - 3\eta) - (2/3 + 3\eta/8)(1 - 2\eta)\right]$$

$$P^2 = \frac{k_\parallel^2 V_A^2}{\omega^2}(1 + \eta/2)$$

If we further neglect the effect of $k_\parallel$ (i.e. $k_\parallel = 0$), we can write the ratio A/B

$$A/B = \frac{\eta}{4\beta_D} \frac{1/3 + \eta/4}{(1 + \eta/2)\left(\frac{5}{6} - \frac{17\eta}{24} + \frac{3\eta^2}{16}\right)}$$

thus showing that the dominant term in the separation of the two regimes is η/β_D. If the plasma also contains a V^{21+} impurity ion of very low concentration ($n_{V^{21+}} < 10^{-3} n_e$), it is then clear that the mode conversion processes, both at the location of the vanadium ion second harmonic and also at the hybrid resonance between hydrogen and vanadium ions (Takahashi's criterium [31]), do not occur.

REFERENCES

ACHARD, M.H., ADAM, J., ANABITARTE, E., ANDREOLETTI, J., BANNELIER, P., BARKLEY, H., BRETON, C., BRETON, J., BRUGNETTI, R., CAPES, H., CHARET, M., CHATELIER, M., COHEN, A., COTSAFTIS, M., CRENN, J.P., DE GENTILE, B., DE MICHELIS, C., DRAWIN, H., DRUAUX, J., DUBOIS, M., FIDONE, I., FOIS, M., GAMBIER, D., GERAUD, A., GERVAIS, F., GIOVANNONI, P., GIRUZZI, G., GROSMAN, A., HECQ, W., HUTTER, T., JACQUET, L., JOHNER, J., KRIVENSKI, V., KUSS, H., LASALLE, J., LAURENT, L., LECOUSTEY, P., LINET, F., MARTIN, G., MATTIOLI, M. OLIVAIN, J., PAIN, M., PLATZ, P., PECQUET, A.L., QUEMENEUR, A., RAMETTE, J., REBUFFI, L., REVERDIN, C., ROUBIN, J.P., SAMAIN, A., SAOUTIC, B., SIMONET, F., SOUBARAS, R., TACHON, J., TOUCHE, J., TOURNESAC, B., TUSZEWSKI, M., VERON, D., ZANFAGNA, B.

[1] COLESTOCK, P.L., IEEE Trans. Plasma Sci. 12 (1984) 64.

[2] EQUIPE TFR, in Heating in Toroidal Plasmas (Proc. 4th Intern. Conf., Rome, 1984), C.C.E. : Brussels, 1 (1984) 277.

[3] EQUIPE TFR, in Plasma Physics and Controlled Nuclear Fusion (Proc. 9th Intern. Conf., Baltimore, 1982) I.A.E.A : Vienna, 2 (1983) 17.

[4] EQUIPE TFR, in Heating in Toroidal Plasmas (Proc. 3th Intern. Conf., Grenoble, 1982), C.E.E. : Brussels, 1 (1982) 225.

[5] TFR GROUP, Nucl. Fusion 22 (1982) 956.

[6] EQUIPE TFR, Plasma Phys. Controlled Fusion 26 (1984) 165.

[7] LONGINOV, A.V., and STEPANOV, K.N., in Heating in Toroidal Plasmas (Proc. 4th Intern. Conf., Rome, 1982), C.C.E. : Brussels, 1 (1984) 489.

[8] LONGINOV, A., PAVLOV, S.S., and STEPANOV, K.N., in Controlled Fusion and Plasma Physics (Proc. 12th Europ. Conf., Budapest, 1985), Europhysics Conf. Abstracts, 2 (1985) 132.

[9] MARMAR, E.S., CECCHI, J.L., and COHEN, S.A., Rev. Sci. Instrum. 46 (1975) 1149.

[10] TFR GROUP, Phys. Lett. 87A (1982) 169.

[11] ALIKAEV, V.V., BEREZOVSKIJ, E.L., VASIN N.A., VDOVIN, V.L., VERTIPOROKH, A.N., et al., in Controlled Fusion and Plasma Physics (Proc. 12th Europ. Conf., Budapest, 1985), Europhysics Conf. Abstracts, 2 (1985) 156.

[12] EQUIPE TFR, Plasma Phys. 24 (1982) 615.

[13] EQUIPE TFR, in Plasma Physics and Controlled Nuclear Fusion Research (Proc. 10th Intern. Conf. London 1984), I.A.E.A. : Vienna, 1 (1985) 103.

[14] BRETON, C., DE MICHELIS, C., HECQ, W., MATTIOLI, M., RAMETTE, J., and SAOUTIC, B., Plasma Phys. Controlled Fusion 27 (1985) 355.

[15] TFR GROUP, Phys. Lett. 112A (1985) 29.

[16] TFR GROUP, Nucl. Fusion 25 (1985) n°12 (in press).

[17] TFR GROUP, Nucl. Fusion 23 (1983) 559.

[18] JACQUINOT, J., and LAPIERRE, Y., in Heating in Toroidal Plasmas (Proc. 2nd Intern. Conf., Como, 1980), C.C.E. : Brussels, 1 (1980) 541.

[19] LAPIERRE, Y., "Chauffage cyclotronique ionique dans le Tokamak de Fontenay-aux-Roses", Thèse de Doctorat d'Etat, Paris-Orsay (1982), and Fontenay-aux-Roses Laboratory Internal Report EUR-CEA-FC 1149 (1982).

[20] KRAPCHEV, V.B., Nucl. Fusion 25 (1985) 455.

[21] GAGEY, B., LAPIERRE, Y., and MARTY, D., in Heating in Toroidal Plasmas (Proc. 3rd Intern. Conf., Grenoble, 1982), C.C.E. : Brussels, 1 (1982) 361.

[22] TRUBNIKOV, B.A., in "Reviews of Plasma Physics" (Leontovich, M.A., ed.), Consultants Bureau : New York, 1 (1965) 105.

[23] SPITZER, L. Jr., "Physics of fully ionized gases", Interscience Publishers (1962).

[24] TFR GROUP, Nucl. Fusion 22 (1982) 1173.

[25] EQUIPE TFR, in Heating in Toroidal Plasmas (Proc. 3rd. Intern. Conf., Grenoble, 1982), C.C.E. Brussels, 3 (1982) 1177.

[26] TFR GROUP, Plasma Phys. Controlled Fusion 26 (1984) 1141.

[27] HWANG, D.Q., HOSEA, J., THOMSON, H., WILSON, J.R., DAVIS, S., et al., Phys. Rev. Lett. 51 (1983) 1865.

[28] ODAJIMA, K., MATSUMOTO, H., KIMURA, H., HOSHINO, K., KASAI, S., et al, in Heating in Toroidal Plasmas (Proc. 4th Intern. Conf., Rome, 1984), C.C.E. : Brussels 1 (1984) 243.

[29] GAMBIER, D.J., and SWANSON D.G., Phys. Fluids 28 (1985) 145.

[30] GAMBIER, D.J., "Etude théorique et expérimentale du chauffage cyclotronique ionique sur le Tokamak TFR", Thèse de Doctorat d'Etat, Paris-Orsay (1985) (unpublished).

[31] TAKAHASHI, H., J. Physique (Colloque C6) 38 (1977) C6-171.

FIGURE CAPTIONS

Figure 1 Central deuteron temperature $T_D(0)$ behaviour during ICR heating. a) inconel environment ; b) carbon environment (P_{RF} = 300 kW, η_H = 0.2, B_T = 4.5 T).

Figure 2 a) Radial profiles of n_e (from HCN laser interferometry), T_e (from Thomson scattering, averaging over a sawtooth), and T_D (from charge-exchange deuteron energy analysis) during ICR heating steady state conditions. b) Radial profiles of vanadium ion densities n_Z, 20 ms after the injection (from the impurity transport code) ; the n_Z values for V^{14+} to V^{17+} ions have been multiplied by 10.

Figure 3 A) Central deuteron temperature $T_D(0)$ evolution (a, from neutrons ; b, from charge exchange deuteron energy analysis). The arrow shows the time of V injection (20 ms before the RF pulse), and the 100 ms RF pulse is hatched (P_{RF} = 600 kW). 1) V injection without ICR heating ; 2) with RF pulse, but no V injection ; 3) with both V injection and RF pulse. B) Same as A, but V injection (shown by the arrow) occurs 20 ms after the RF pulse application.

Figure 4 $f_{2cZ}/2f_{CH} = Z/A$ for highly-ionized ions of different atomic species of charge Z_N (upper abscissa scale and left ordinate scale) ; ● fully-stripped ions ; ■ H-like ions ; * He-like ions ; ▲ Li-like ions ; ◀ Be-like ions. $f_{Hy}/2f_{cH}$ for a three-ion plasma as a function of $n_{C^{6+}}$ (= $n_{C^{6+}}/n_D$) for two different η_H (= n_H/n_D) values (thick solid lines, lower abscissa scale and right ordinate scale).

Figure 5 Influence on the dispersion curve $k_x = f(x)$ of the values of $k_{\parallel}$, $n_{C^{6+}}$, and y (height above the mid-plane). Solid line : reference case ($k_{\parallel} = 6m^{-1}$, $n_{C^{6+}} = 10^{-4}$, y = 0.1 cm) ; dotted line : increased $n_{C^{6+}}$ value ($n_{C^{6+}} = 3\ 10^{-2}$) ; dot-dashed line : increased $k_{\parallel}$ value ($k_{\parallel} = 8m^{-1}$) ; dashed line : increased y value (y = 2 cm). The V^{21+} resonance layer position R_{V21+} is also shown. B_T = 4.5 T, η_H = 0.2, $n_{V^{21+}} = 10^{-3}$, $n_{V^{20+}} = 5\ 10^{-4}$.

Figure 6 a) $\mathrm{Log}_{10}\ k_i$ as a function of x for two V ions and electrons ; b) integrated fractional fast wave absorbed power $P_a(x)$. B_T = 4.5 T, n_H = 0.2, $n_{C^{6+}}$ = 3 10^{-2}, $k_{\parallel}$ = 6 m^{-1}, y = 0.1 cm. The dot-dashed and solid lines are for the fast and slow waves, respectively : $n_{V^{21+}}$ = 5 10^{-4}, $n_{V^{20+}}$ = 2.5 10^{-4}, $\alpha = T_V/T_D$ = 40 for both ions. The dotted and dashed lines are for the fast and slow waves, respectively : $n_{V^{21+}}$ = 5 10^{-4}, $n_{V^{20+}}$ = 2.5 x 10^{-4}, α = 1 for both slow populations, whereas $n_{V^{21+}}$ = 5 x 10^{-5}, $n_{V^{20+}}$ = 2.5 10^{-5}, α = 40 for the fast populations.

Figure 7 Integrated fractional absorbed power P_a as a function of x for electrons and V^{21+} ions at two different heights y above the mid-plane. Other parameters : same as in figure 6 with two V ion fast populations ($n_{V^{21+}}$ = 10^{-3}, $n_{V^{20+}}$ = 5 10^{-4}, α = 40)

Figure 8 Total integrated fractional power $P_a(\infty)$ absorbed by V^{21+} ions versus $k_{\parallel}$ at three different heights y above the mid-plane. Other parameters : same as for the solid lines in figure 7.

Figure 9 Solid line : power per unit V^{21+} ion that can be coupled to deuterons via Coulomb collisions as a function of the V^{21+} ions temperature T_V. Dashed line : same as the solid line but for C^{5+} ions with temperature T_C.

Figure 10 Radial profiles of central Ni ion densities (specified by the isoelectronic sequence), as given by the impurity transport simulation code at the time of maximum $T_D(0)$ value, during ICR heating at B_T = 4.9 T.

Figure 11 a) Dispersion equation $k_x = f(x)$ for 4 values of n_H and $k_{\parallel}$ = 6 m^{-1}, b) total integrated fractional absorbed powers $P_a(\infty)$ as a function of k for the same n_H values. $n_e(0)$ = 1.8 x 10^{14} cm^{-3}, $T_e(0)$ = 1.6 keV, $T_D(0)$ = 1.2 keV, B_T = 4.9 T, $\alpha = T_{Ni}/T_D$ = 40 ; $n_{C^{6+}}$ = 1.2 x 10^{-2} ; $n_{Ni^{26-}}$ = 2 x 10^{-5}, $n_{Ni^{25+}}$ = 6 x 10^{-5}, $n_{Ni^{24-}}$ = 10^{-4} ; $n_{Ni^{23+}}$ = 1.5 x 10^{-4}. The Ni ion resonance layers (a) and the absorbing Ni ions (b) are specified by the isoelectronic sequence.

Figure 12 a) Increase of the central deuteron temperature $T_D(0)$ from neutron diagnostics as a function of η_H (P_{RF} = 650 kW, B_T = 4.9 T). b) Initial rate of increase of the central deuteron temperature $dT_D(0)/dt$ at the RF pulse application in the same experiments.

TABLE 1

Energy-exchange time $\tau(V^{21+},i)$ in μs for the slowing-down process of a V^{21+} test particle in an assembly of deuterons, protons, fully-ionized C^{6+} ions, partially-stripped V^{21+} ions and electrons (densities in cm^{-3}, temperatures in eV).

$E_{V^{21+}}$	D^+ $n_D = 10^{14}$ $T_D = 1200$	C^{6+} $n_{C^{6+}} = 2\ 10^{12}$ $T_{C^{6+}} = 1200$	H^+ $n_H = 2\ 10^{13}$ $T_H = 1200$	V^{21+} $n_{V^{21+}} = 4\ 10^{10}$ $T_{V^{21+}} = 1200$	e $n_e = 1.2\ 10^{14}$ $T_e = 1700$
Equipartition	18	14	110		630
10 keV	26	32	170	350	800
40 keV	36	170	170	2800	690

S C P

ÉQUIPE T.F.R.

LISTE N° 12 - MISE À JOUR DU 1ER. OCTOBRE 1985

EXPLOITATION PHYSIQUE DE L'EXPÉRIENCE

- COORDINATION	M. CHATELIER J. TACHON
- SECRÉTARIAT SCIENTIFIQUE	P. LECOUSTEY
- CONDUITE DE LA MACHINE	P. BANNELIER M. CHATELIER M. DUBOIS P. GIOVANNONI L. LAURENT
- MESURES MAGNÉTIQUES	P. LECOUSTEY
- INTERFÉROMÉTRIE HCN	D. VERON
- RÉFLECTOMÉTRIE	F. ANABITARTE F. SIMONET
- DIFFUSION THOMSON	J. LASALLE B. PLAIZ
- SPECTRES DE NEUTRES	T. HUTTER C. REVERDIN
- MESURES NUCLÉAIRES, X-DURS	A. GERAUD G. MARTIN
- RAYONS X-MOUS	L. JACQUET A.L. PECQUET
- SPECTROMÉTRIE (VISIBLE, UV, X-MOUS)	C. BRETON C. DE MICHELIS W. HECQ M. MATTIOLI P. PLAIZ J. RAMETTE B. SAOUTIC
- SPECTROMÉTRIE DE MASSE, CONDITIONNEMENT DES PAROIS, PLASMA PÉRIPHÉRIQUE, BOLOMÉTRIE	M.H. ACHARD A. GROSMAN F. LINET
- RAYONNEMENT CYCLOTRONIQUE ELECTRONIQUE A/ SPECTROMETRIE INFRAROUGE B/ ÉTUDES MICROONDES	L. LAURENT R. SOUBARAS B. ZANFAGNA
- MESURES DE LA TURBULENCE PAR DIFFUSION THOMSON	H. BARKLEY B. DE GENTILE F. GERVAIS J. OLIVAIN A. QUEMENEUR
- INJECTION DE GLACONS	H. DRAWIN A. GERAUD

./...

CHAUFFAGES ADDITIONNELS

- INJECTION DE NEUTRES.....	J. DRUAUX M. FOIS P. GIOVANNONI J.P. ROUBIN
- CHAUFFAGE CYCLOTRONIQUE ELECTRONIQUE.....	J.P. CRENN M. DUBOIS L. REBUFFI B. TOURNESAC M. TUSZEWSKI B. ZANFAGNA
- CHAUFFAGE CYCLOTRONIQUE IONIQUE.....	J. ADAM P. BANNELIER R. BRUGNETTI D. GAMBIER H. KUUS

INFORMATIQUE

- MATÉRIEL.....	M. CHAREI
- LOGICIEL.....	J. BREION A. COHEN C. REVERDIN J. TOUCHE

THÉORIE .....

J. ANDREOLEITI
H. CAPES
M. DUBOIS
I. FIDONE
G. GIRUZZI
V. KRIVENSKI
M. PAIN
A. SAMAIN

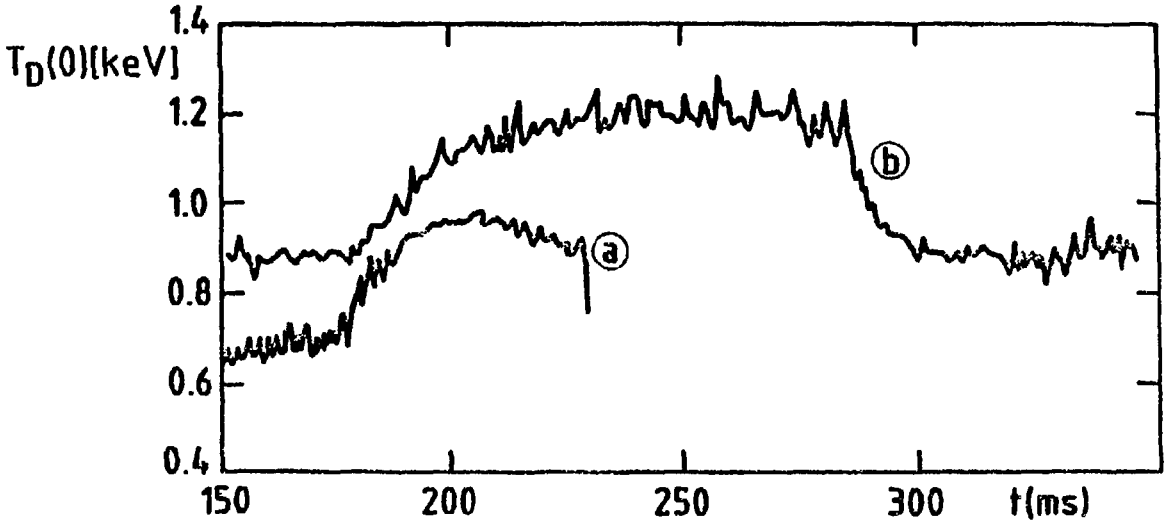

Fig. 1

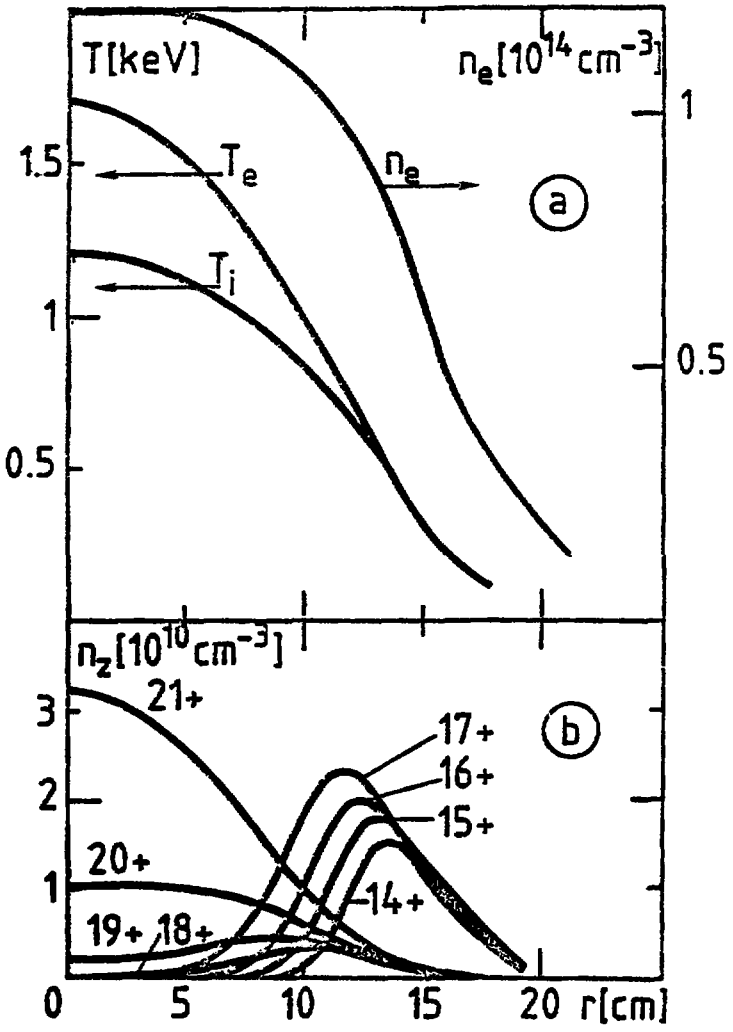
T[keV]
$n_e[10^{14}cm^{-3}]$
1.5
1
0.5
T_e
T_i
n_e
a
1
0.5
$n_z[10^{10}cm^{-3}]$
3
2
1
21+
20+
19+
18+
17+
16+
15+
14+
b
0
5
10
15
20
r[cm]

Fig. 2

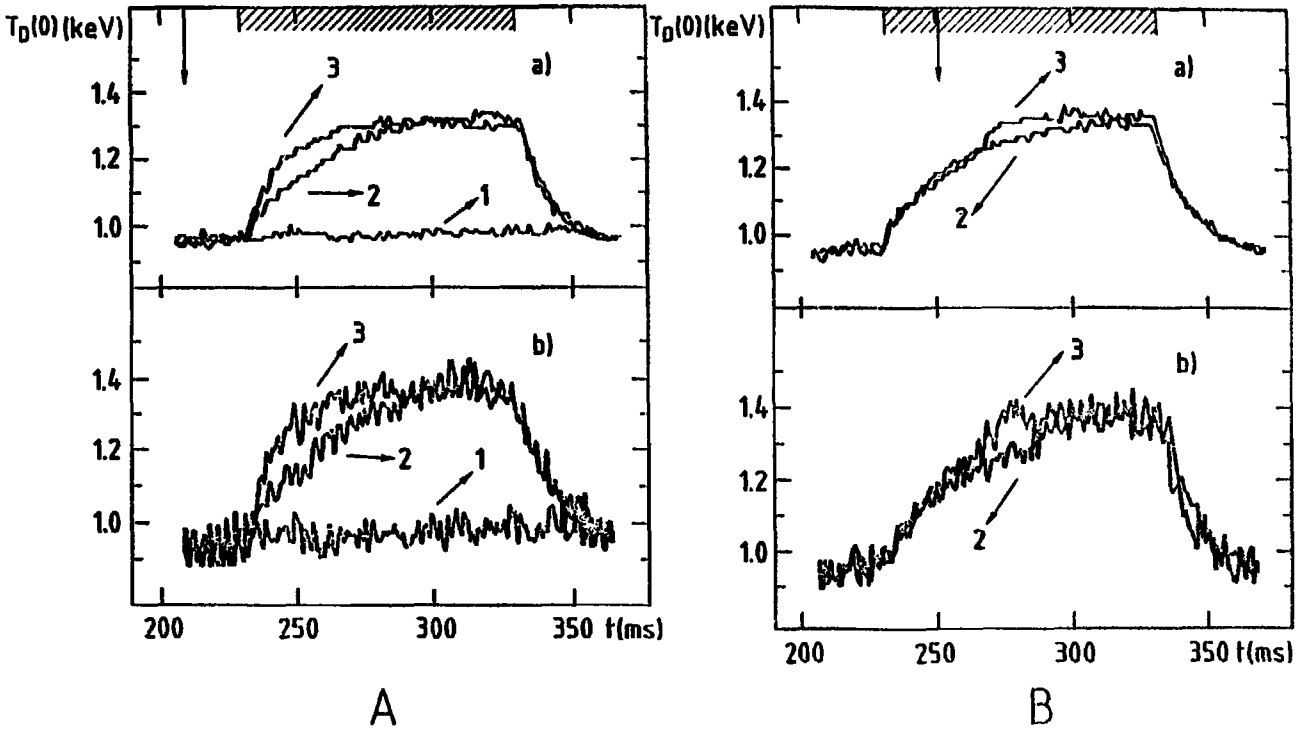

Fig. 3

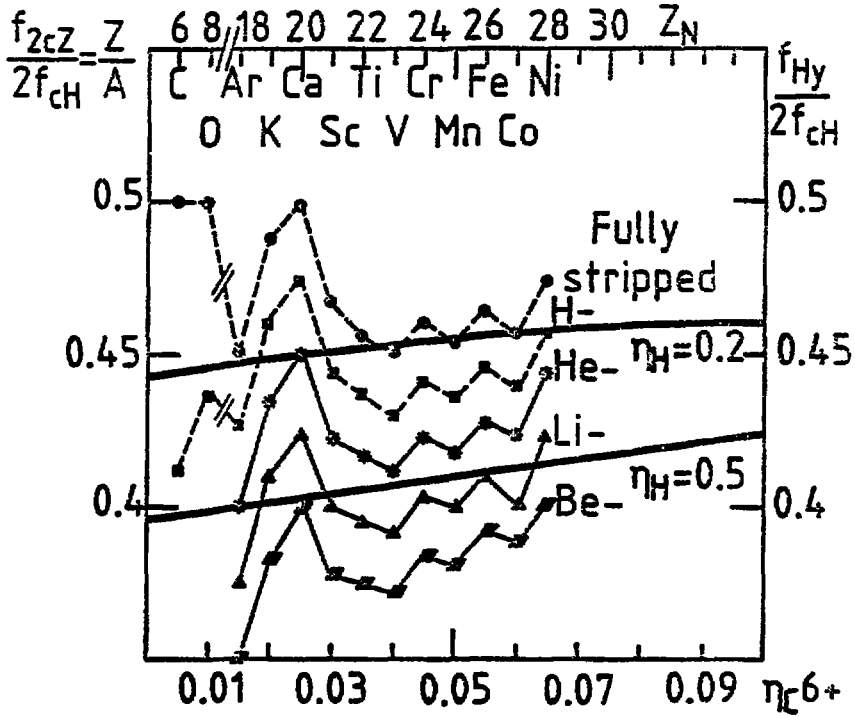
$\frac{f_{2cZ}}{2f_{cH}}=\frac{Z}{A}$
6 8 18 20 22 24 26 28 30 Z_N
C Ar Ca Ti Cr Fe Ni
O K Sc V Mn Co
$\frac{f_{Hy}}{2f_{cH}}$
0.5
0.45
0.4
Fully stripped
H-
He-
Li-
Be-
η_H=0.2
η_H=0.5
0.01 0.03 0.05 0.07 0.09 $\eta_{C^{6+}}$

Fig. 4

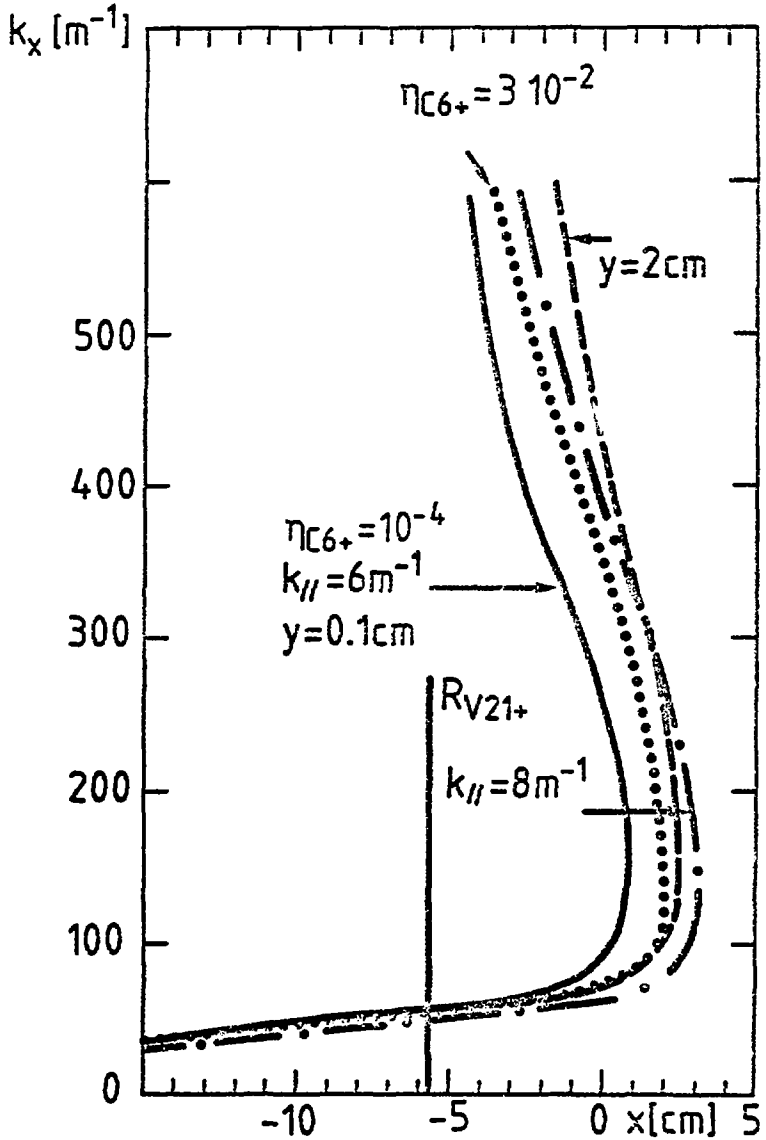
k_x [m^{-1}]
$n_{C6+}=3\ 10^{-2}$
y=2cm
500
400
$n_{C6+}=10^{-4}$
$k_{//}=6m^{-1}$
y=0.1cm
300
R_{V21+}
$k_{//}=8m^{-1}$
200
100
0
-10
-5
0 x[cm] 5

Fig. 5

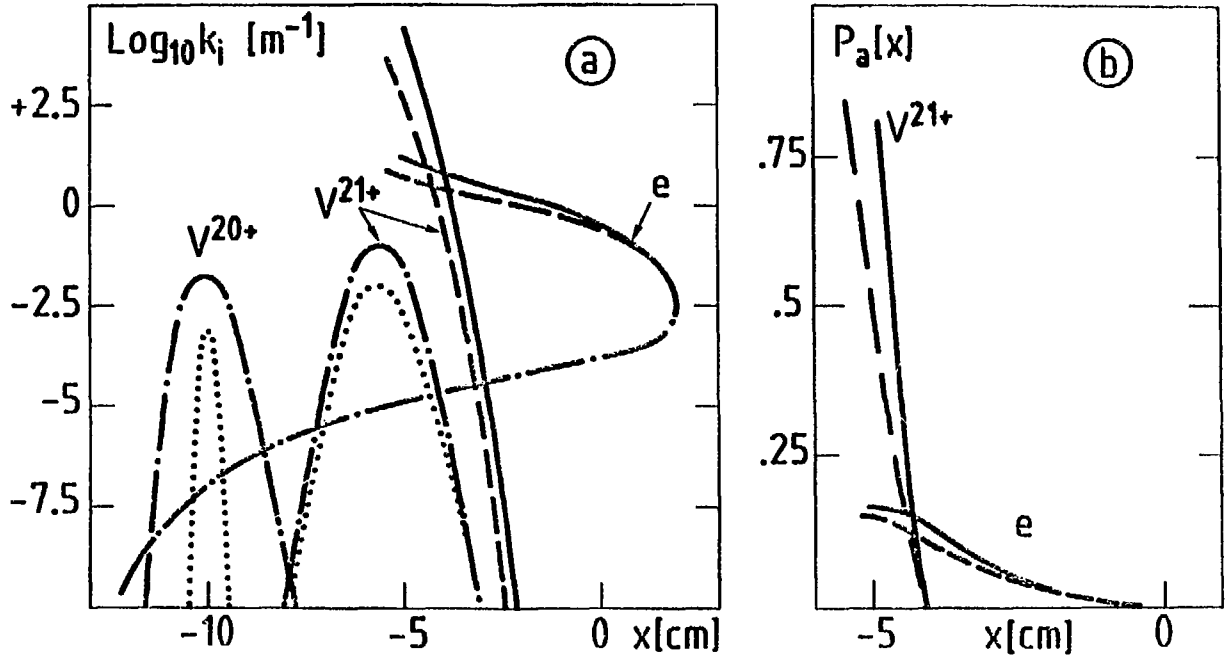
Log10ki [m-1]
a
+2.5
0
-2.5
-5
-7.5
V20+
V21+
e
-10
-5
0 x[cm]
Pa[x]
b
.75
.5
.25
V21+
e
-5
x[cm]
0

Fig. 6

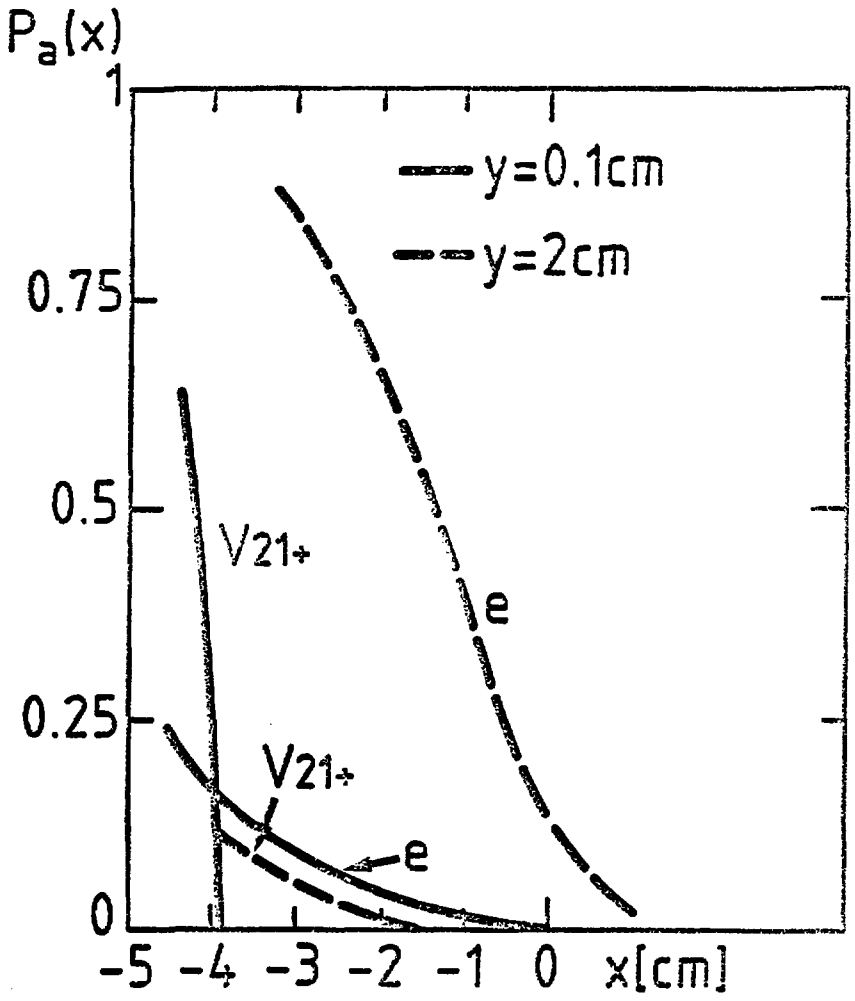

Fig. 7

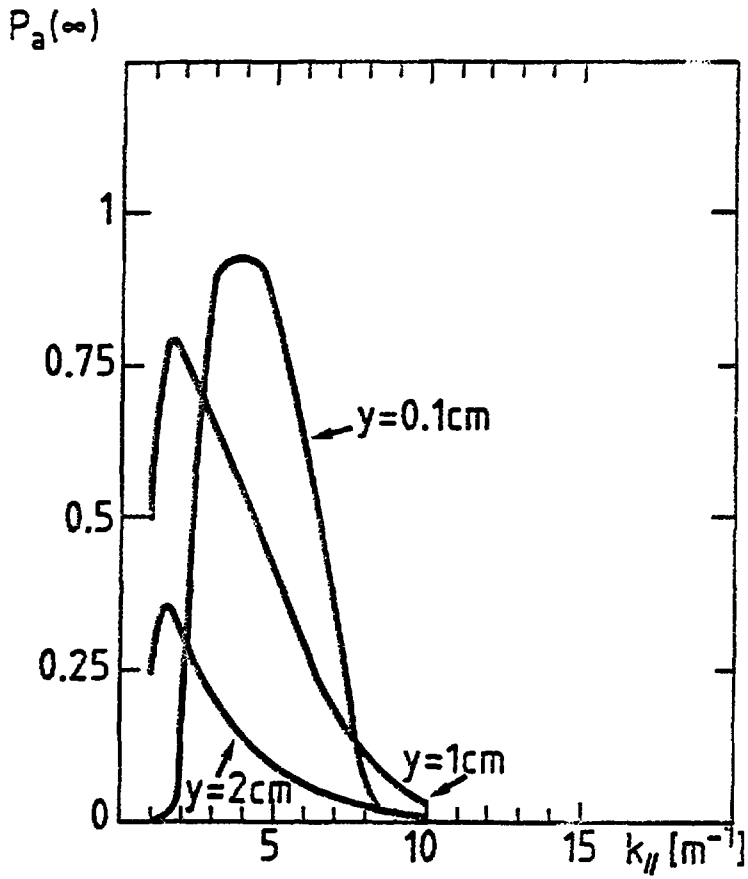

Fig. 8

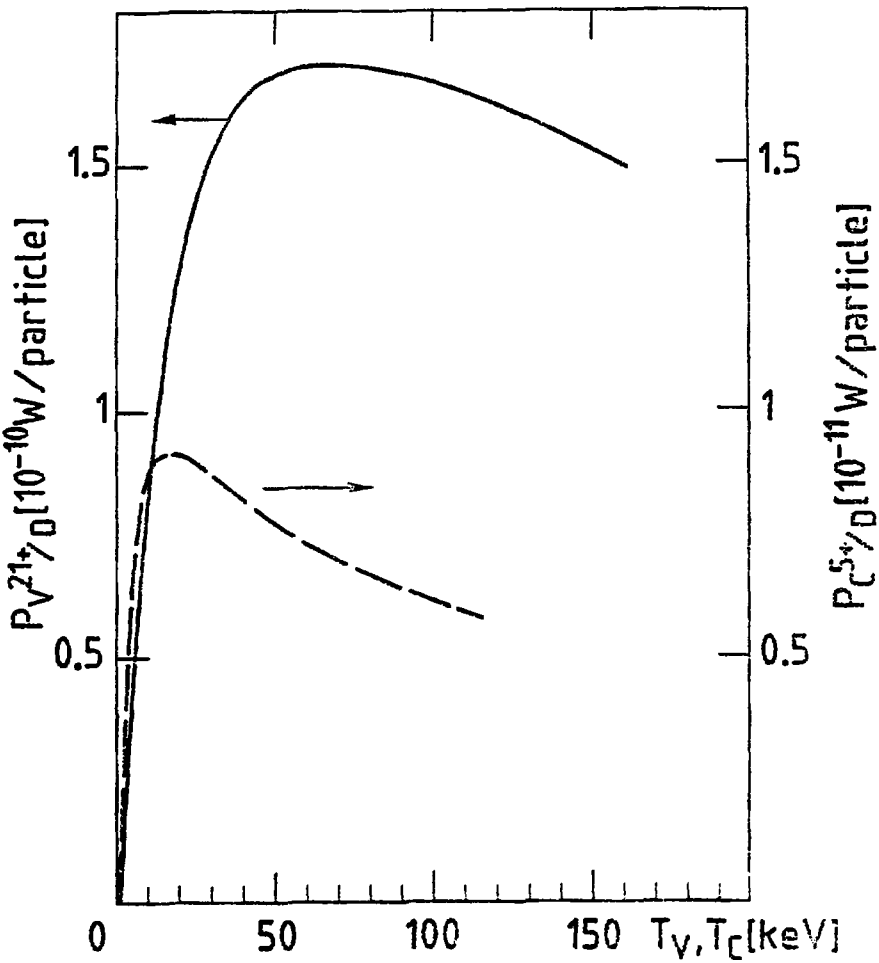
1.5
1
0.5
0
50
100
150
T_V, T_C[keV]
$P_V^{21+}/_D$[10^{-10}W/particle]
$P_C^{5+}/_D$[10^{-11}W/particle]

Fig. 9

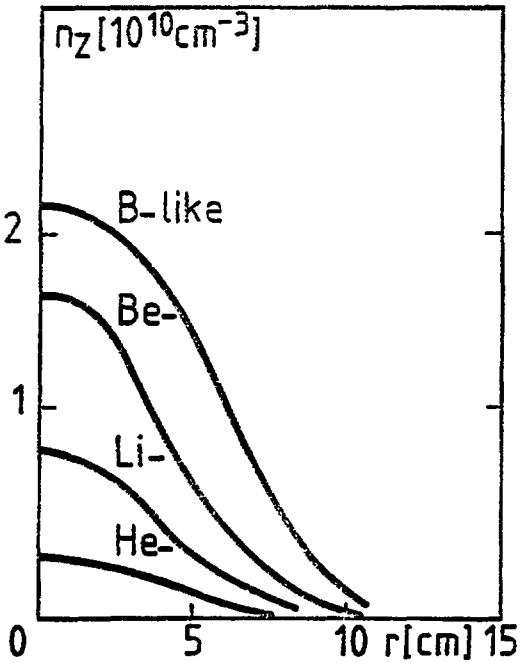

Fig. 10

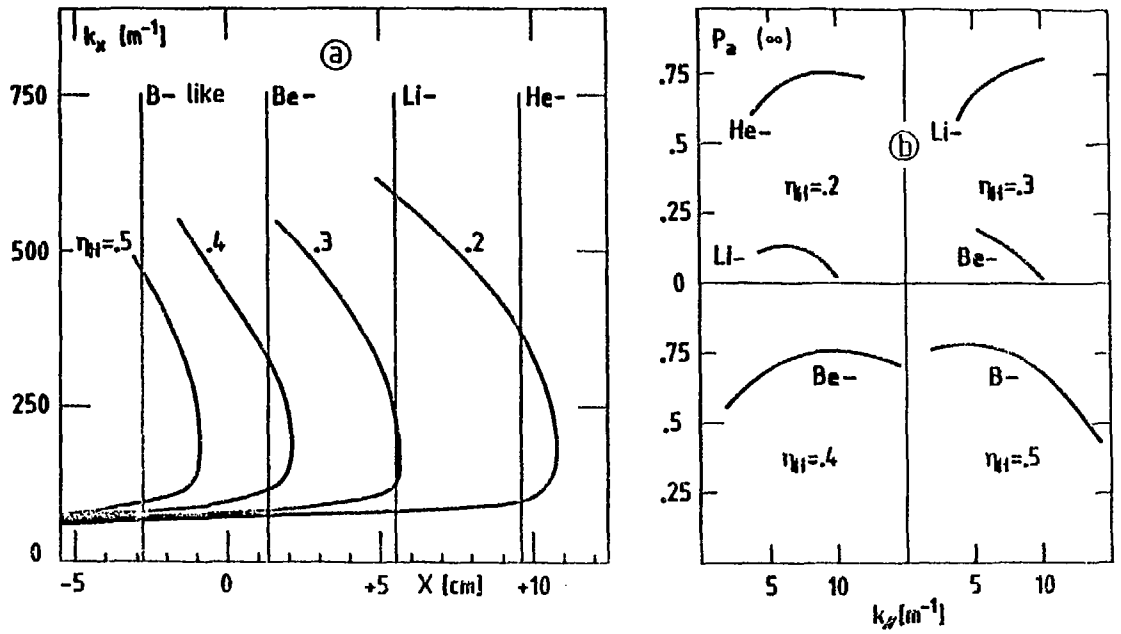
k_x (m^-1)
ⓐ
750
500
250
0
B- like
Be-
Li-
He-
η_H=.5
.4
.3
.2
-5
0
+5
X (cm)
+10
P_a (∞)
.75
.5
.25
0
He-
ⓑ
Li-
η_H=.2
η_H=.3
Li-
Be-
Be-
B-
η_H=.4
η_H=.5
5
10
5
10
k_y (m^-1)

Fig. 11

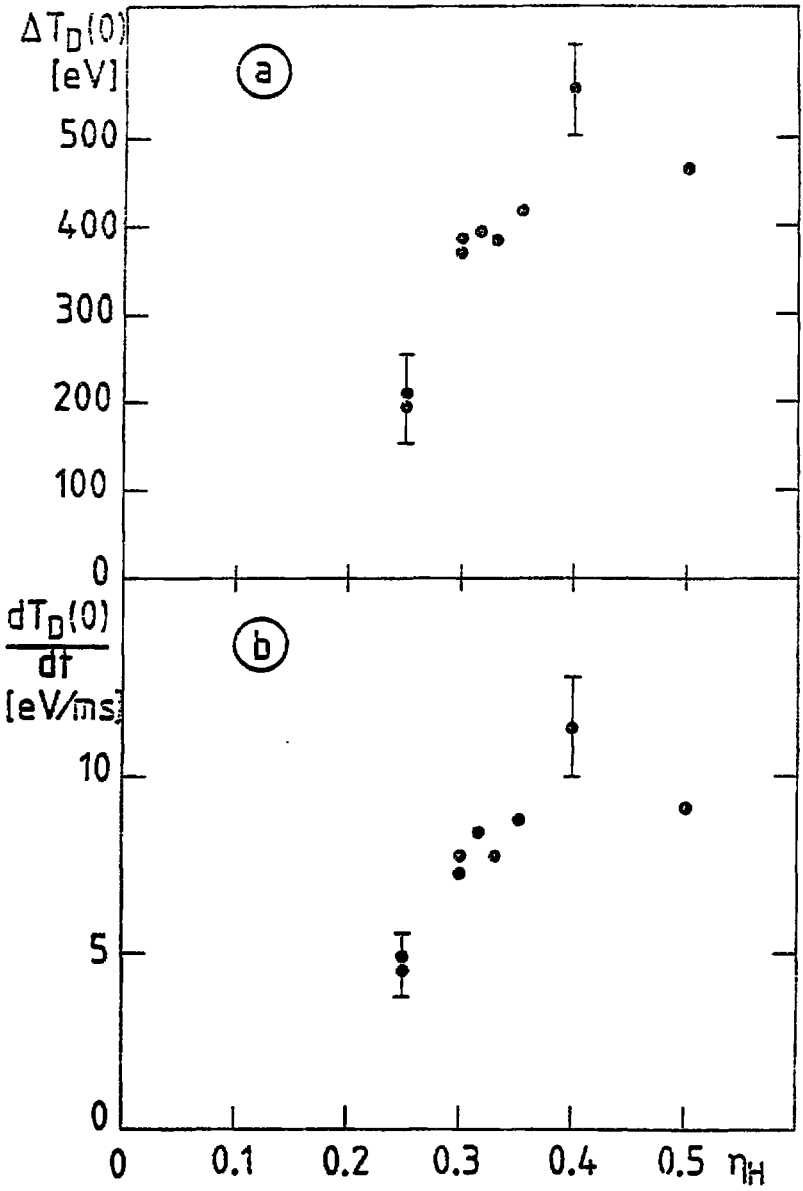
ΔT_D(0)
[eV]
a
500
400
300
200
100
0
dT_D(0)/dt
[eV/ms]
b
10
5
0
0
0.1
0.2
0.3
0.4
0.5
η_H

Fig. 12